Published in final edited form as:
Toxicol Appl Pharmacol. 2013 October 15; 272(2): 299–305. doi:10.1016/j.taap.2013.06.016.

Small heterodimer partner overexpression partially protects against liver tumor development in farnesoid X receptor knockout mice

Guodong Li[1,*], **Bo Kong**[2,*], **Yan Zhu**[3], **Le Zhan**[2,4], **Jessica A. Williams**[4], **Ossama Tawfik**[5], **Karen M. Kassel**[4], **James P. Luyendyk**[6], **Li Wang**[7], and **Grace L. Guo**[2]

[1]Department of Surgical Oncology, Cancer treatment center, The Fourth Affiliated Hospital of Harbin Medical University, Harbin, China

[2]Department of Pharmacology and Toxicology, School of Pharmacy, Rutgers University, Piscataway, NJ, USA

[3]Department of General Surgery, Xuanwu Hospital, Capital Medical University, Beijing, China

[4]Department of Pharmacology, Toxicology and Therapeutics, University of Kansas Medical Center, Kansas City, KS, USA

[5]Department of Pathology and Laboratory Medicine, University of Kansas Medical Center, Kansas City, KS, USA

[6]Pathobiology and Diagnostic Investigation, Michigan State University, East Lansing, MI, USA

[7]Department of Medicine, Huntsman Cancer Institute, University of Utah School of Medicine, Salt Lake City, UT, USA

Abstract

Farnesoid X receptor (FXR, *Nr1h4*) and small heterodimer partner (SHP, *Nr0b2*) are nuclear receptors that are critical to liver homeostasis. Induction of SHP serves as a major mechanism of FXR in suppressing gene expression. Both $FXR^{-/-}$ and $SHP^{-/-}$ mice develop spontaneous hepatocellular carcinoma (HCC). SHP is one of the most strongly induced genes by FXR in the liver and is a tumor suppressor, therefore, we hypothesized that deficiency of SHP contributes to HCC development in the livers of $FXR^{-/-}$ mice and therefore, increased SHP expression in $FXR^{-/-}$ mice reduces liver tumorigenesis. To test this hypothesis, we generated $FXR^{-/-}$ mice with overexpression of SHP in hepatocytes ($FXR^{-/-}/SHP^{Tg}$) and determined the contribution of SHP in HCC development in $FXR^{-/-}$ mice. Hepatocyte-specific SHP overexpression did not affect liver tumor incidence or size in $FXR^{-/-}$ mice. However, SHP overexpression led to a lower grade of dysplasia, reduced indicators cell proliferation and increased apoptosis. All tumor-bearing mice

Corresponding author: Grace L. Guo, Ph.D., Department of Pharmacology and Toxicology, School of Pharmacy, Rutgers University, Piscataway, NJ, USA. 08854 Phone: +1 913-904-8224; guo@eohsi.rutgers.edu.
*These two authors contribute equally.

had increased serum bile acid levels and IL-6 levels, which was associated with activation of hepatic STAT3. In conclusion, SHP partially protects $FXR^{-/-}$ mice from HCC formation by reducing tumor malignancy. However, disrupted bile acid homeostasis by FXR deficiency leads to inflammation and injury, which ultimately results in uncontrolled cell proliferation and tumorigenesis in the liver.

Keywords

farnesoid X receptor; small heterodimer partner; tumor malignancy; bile acids; chronic injury; liver tumor

Introduction

Hepatocellular carcinoma (HCC) accounts for 85% of primary liver cancers and represents a major health problem worldwide for its high prevalence and poor prognosis. Chronic viral infections and hepatotoxic agents are the major risk factors contributing to HCC etiology. Although common pathological changes in HCC are well characterized, which consist of intertwined chronic injury and inflammation, the precise molecular mechanisms underlying HCC development are still unclear (Li and Guo, 2011). Emerging evidence strongly indicate that the molecular pathogenesis of HCC is multi-faceted (El-Serag, 2011, and increase in bile acids promotes HCC formation in rodents {Cameron, 1981 #2797) and is associated with HCC development in humans (Chen et al., 2011).

Farnesoid X receptor (FXR, *Nr1h4*) and small heterodimer partner (SHP, *Nr0b2*) are ligand-activated nuclear receptors (NRs) and are important in regulating liver functions, including bile acid metabolism, lipid homeostasis, drug disposition, inflammation, cell growth and differentiation, and tumorigenesis (Zhang et al., 2011; Zhu et al., 2011). Bile acids are endogenous ligands of FXR and FXR is essential in regulating bile acid homeostasis (Makishima et al., 1999; Parks et al., 1999; Sinal et al., 2000; Wang et al., 1999). Increase in bile acids causes liver injury, which may serve as one of the mechanisms of HCC formation in $FXR^{-/-}$ mice by activating cell proliferating pathways, such as β-catenin (Wolfe et al., 2011). Furthermore, liver injury leads to increased IL-6 levels, which can activate STAT3, and STAT3 activation is a well-known mechanism responsible for liver carcinogenesis (Yu et al., 2009). Emerging evidence showed FXR deficiency led to STAT3 activation (Meng et al., 2012; Xu et al., 2012), indicating that STAT3 activation may also be involved in liver carcinogenesis with FXR deficiency.

SHP is highly induced by FXR activation in the liver (Li et al., 2010), and both $FXR^{-/-}$ and $SHP^{-/-}$ mice develop spontaneous HCC (Kim et al., 2007; Yang et al., 2007; Zhang et al., 2008). Increasing evidence indicates that SHP possesses potent tumor-suppressive activity by inhibiting cell proliferation and promoting apoptosis (He et al., 2008; Zhang et al., 2010; Zhang et al., 2008). However, the mechanisms whereby FXR suppresses liver carcinogenesis are not completely clear. Understanding the mechanisms will provide critical scientific basis to help understand HCC carcinogenesis, which may be used to improve the HCC therapeutic strategy. Therefore, we hypothesize that deficiency of SHP contributes to HCC development in $FXR^{-/-}$ mice and increase in SHP expression in $FXR^{-/-}$ mice reduces

liver tumorigenesis. In the current study, we have generated $FXR^{-/-}/SHP^{Tg}$ mice in which SHP was overexpressed in hepatocytes of $FXR^{-/-}$ mice. With this unique mouse model, we have determined the contribution of SHP to liver tumor development in $FXR^{-/-}$ mice.

Materials and Methods

Animals and treatments

All mice were housed and bred in pathogen-free animal facilities in the Laboratory of Animal Research under a standard 12-hr light/dark cycle with free access to food and autoclaved tap water. All protocols and procedures were approved by the Institutional Animal Care and Use Committee (IACUC) at the University of Kansas Medical Center. Four mouse strains in C57BL/6J genetic background were bred in house and used in this study: wild-type (WT), $FXR^{-/-}$, SHP-hepatocyte transgenic (SHP^{Tg}) and $FXR^{-/-}/SHP^{Tg}$ mice. The $FXR^{-/-}/SHP^{Tg}$ mice were created by cross-breeding $FXR^{-/-}$ and SHP^{Tg} mice. For genotyping, tail DNA extraction and standard PCR amplification were performed using a Sigma RED Extract-N-Amp Tissue PCR Kit obtained from Sigma-Aldrich (St. Louis, MO). The sequence of the primers used for genotyping the FXR allele and SHP transgenic allele were presented in supplemental table 1. Both male and female mice were sacrificed at 3, 6, 12 and 18 months of age with n=14–20/gender/genotype/time point.

Mouse liver tissue processing

Liver tissues were either snap-frozen in liquid nitrogen followed by RNA and protein preparations or fixed in 4% formaldehyde-PBS solution, embedded in paraffin, and cut into 5-μm sections for hematoxylin and eosin (H&E) staining or immunohistochemistry. The pathology analysis was performed by Dr. Ossama Tawfik who is a board-certified pathologist with liver experience at the Department of Pathology and laboratory of Medicine at the University of Kansas Medical Center.

5-bromo-2-deoxyuridine (BrdU) staining

To assess liver cell proliferation, 3- and 12-month-old WT, $FXR^{-/-}$, SHP^{Tg}, and $FXR^{-/-}/SHP^{Tg}$ mice were injected intraperitoneally with 50 mg/kg of BrdU (BD Biosciences, San Jose, CA) in PBS daily for 5 days. The livers were harvested 2 hrs after the last injection. BrdU staining results were quantitated by assessing at least 1000 cells per tissue section to calculate the percentage of positive nuclei (brown nuclei) at 400×magnification.

Terminal deoxynucleotidyl transferase-mediated dUTP nick-end labeling (TUNEL) assay

To determine cell apoptosis, the TUNEL assay was performed on liver sections using a TUNEL kit (In Situ Cell Death Detection Kit AP, Roche Diagnostics, Indianapolis, USA) according to the manufacturer's recommendations. The numbers of apoptotic hepatocytes were counted in 10 randomly chosen 400X magnification fields using an Olympus BX51 microscope (Hitschfel Instruments, Inc., St. Louis, MO), and the apoptotic TUNEL index was determined as number of apoptotic cells per 1000 cells (‰).

Arginase 1 Immunohistochemistry staining

Immunohistochemistry for arginase 1 was performed using a rabbit polyclonal antibody against arginase-1 (H-52: sc-20150, Santa Cruz, TX) at 1:100 dilution with a labeled streptavidin- biotin-peroxidase complex technique. Briefly, liver tissue sections were deparaffinized and hydrated in xylene and descending grades of alcohol. After rinsing in PBS, antigen retrieval was performed by boring the tissue sections in citrate buffer, pH 6.0 for 10 min. The endogenous peroxidase activity was quenched in 3% hydrogen peroxide for 10 min and endogenous biotin was blocked with avidin/biotin blocking kit (VECTASTAIN, SP-2001) for 30 min before blocking by 5% goat serum for 30min, and subsequently incubated with primary antibody for 1.5 hrs at room temperature. The antibody reaction was detected with the avidin-biotin detection kit using diaminobenzidine (DAB) as chromogen. Sections were counterstained with hematoxylin for 3 min before checked under microscope.

Liver IL-6 levels and serum ALT activity, total bile acids, and IL-6 level

Serum ALT activity and bile acid levels were determined using commercially available kits (Pointe Scientific, Canton, MI and Bio-Quant, San Diego, CA, respectively) according to the manufacturers' instructions. Serum and liver IL-6 levels were measured with a custom Milliplex MAP kit for mouse cytokines (Millipore Corporation, Billerica, MA) using the Bio-Plex 200 System (Bio-Rad Laboratories).

RNA isolation and quantitative real-time PCR (Q-PCR)

Total RNA was isolated from frozen livers by TRIzol reagent. The mRNA expression levels of genes were quantified by Q-PCR using SYBR green chemistry (Fermentas, Glen Burnie, MD) and normalized to *Gapdh* mRNA levels. The names of the genes and the primers are listed in Supplemental Table 1.

Western blot analysis

Proteins were isolated and quantitated by standard method and the Western blot analysis was performed as previously described on total, nuclear and cytoplasmic proteins (Maran et al., 2009). Antibodies are described in Supplemental Table 2.

Statistical analysis

All data were presented as mean ± SD, and were analyzed by one-way analysis of variance followed by the Student-Newman-Keuls test. $P < 0.05$ was considered statistically significant.

Results

Generating $FXR^{-/-}/SHP^{Tg}$ mice—We have generated the $FXR^{-/-}/SHP^{Tg}$ mice in which SHP was overexpressed in hepatocytes of $FXR^{-/-}$ mice. The successful generation of the $FXR^{-/-}/SHP^{Tg}$ mice was confirmed by PCR-based genotyping (Figure 1A) and by measuring mRNA levels of FXR and SHP (Figure 1B). The liver/body weight ratio remained similar among all four strains at 3 and 6 months of age. Starting from 12 months,

the liver/body weight ratio was much higher in the $FXR^{-/-}$ and $FXR^{-/-}/SHP^{Tg}$ mice (Figure 1C).

Overexpression of SHP did not reduce tumor incidence or size, but decreased tumor malignancy—Liver tumor development was examined in WT, $FXR^{-/-}$, SHP^{Tg}, and $FXR^{-/-}/SHP^{Tg}$ mice at 3, 6, 12 and 18 months of age. Grossly identifiable liver tumors were not found in WT or SHP^{Tg} mice at all ages examined, but tumors were found in $FXR^{-/-}$ and $FXR^{-/-}/SHP^{Tg}$ mice at 12 and 18 months of age with no gender difference (Figure 2A). Interestingly, the tumor incidence in FXR −/− mice [9 of 16 (56.3%)] is slightly lower than that in FXR −/−/SHPTg mice [9 of 14 (64.3%)] at 12-month-old age. However, both strains develop 100% tumors at 18-month-old age (Table 1). The overexpression of SHP cannot prevent the tumor development in FXR−/− mice. Liver pathology in 18-month old, tumor-bearing mice included portal and parenchymal inflammation, hepatocellular dysplasias and HCC (Figure 2B), as well as steatosis, bile ductular proliferation, patchy parenchymal necrosis, bile duct adenoma, and bile duct carcinoma (data not shown). As mentioned earlier, the liver/body weight ratio increased dramatically in $FXR^{-/-}$ and $FXR^{-/-}/SHP^{Tg}$, but not in WT and SHP^{Tg} mice at 12 and 18 months of age. However, hepatocellular dysplasias, portal and parenchymal inflammatory cell infiltration were found ~20–40% less in $FXR^{-/-}/SHP^{Tg}$ mice than in $FXR^{-/-}$ mice, indicating that SHP overexpression likely reduces tumor malignancy (Table 2). Arginase immunohistochemistry staining showed that arginase-1 immunostaining was stronger in $FXR^{-/-}$ mouse livers than in $FXR^{-/-}/SHP^{Tg}$ mouse livers at 18-month old (Supplemental Figure 1).

Cell proliferation and apoptosis

Hepatocyte proliferation, assessed by BrdU incorporation, was examined in 3- and 12-month old mice. At 3-month old, BrdU staining markedly increased in $FXR^{-/-}$ and $FXR^{-/-}/SHP^{Tg}$ mice, but not in WT and SHP^{Tg} mice (Figure 2C). At 12 months of age, hepatocyte proliferation was slightly increased only in $FXR^{-/-}$ mice, but not in other strains. We then determined the degree of apoptosis in livers of these mice at 3 and 12 months of age by TUNEL assay (Figure 2D). In agreement with the previous report (Zhang et al., 2010), SHP overexpression increased the degree of apoptosis in both 3- and 12-month old mice. Interestingly, both $FXR^{-/-}$ and $FXR^{-/-}/SHP^{Tg}$ mice markedly increased apoptosis at 3 months of age, but this trend did not continue with aging, as the 12-month old $FXR^{-/-}$ and $FXR^{-/-}/SHP^{Tg}$ mice had a lower degree of apoptosis than the 3-month old mice had, albeit still higher than WT mice at this age.

Serum ALT and BA levels—Both serum ALT activity and bile acid levels were normal in WT and SHP^{Tg} mice in all ages examined, but were markedly increased in $FXR^{-/-}$ and $FXR^{-/-}/SHP^{Tg}$ mice in an age-dependent manner (Figure 3).

Cyclin D1 levels—Cyclin D1 is critical for cell proliferation and has been shown to be a negative target gene of SHP (Zhang et al., 2008). Levels of CyclinD1 mRNA were increased in livers of 12- and 18-month old $FXR^{-/-}$ and $FXR^{-/-}/SHP^{Tg}$ mice, but not in younger mice (Figure 4A). Levels of CyclinD1 protein were determined in livers of 3- and 18-month old

mice, and the results showed that no difference was found at 3-month old, but at 18-month old, $FXR^{-/-}$ and $FXR^{-/-}/SHP^{Tg}$ mice had higher CyclinD1 protein levels (Figure 4B).

Activation of STAT3 in the liver of $FXR^{-/-}$ and $FXR^{-/-}/SHP^{Tg}$ mice—Despite histologic evidence of reduced tumor malignancy in SHP-overexpressing mice, tumor incidence and size was similar in $FXR^{-/-}$ mice regardless of SHP expression levels. This result indicates a cell-proliferative pathway mainly regulated by FXR is responsible for early development of liver tumors. To elucidate the early events during liver carcinogenesis mediated by FXR deficiency, we focused on determining the activation of several signaling pathways that are known to contribute to HCC development in 3-month old mice. STAT3 activation, revealed by Tyr705 and Ser727 phosphorylation, was increased in $FXR^{-/-}$ and $FXR^{-/-}/SHP^{Tg}$ mice, whereas total STAT3 protein levels remained unchanged (Figure 5A). Moreover, phosphorylated JAK2, the up-stream activator of STAT3, was increased in $FXR^{-/-}$ and $FXR^{-/-}/SHP^{Tg}$ mouse livers and decreased in SHP^{Tg} mice (Figure 5A). The protein levels of glycoprotein 130 receptor (GP130), the IL-6 receptor that activates the STAT3 pathway, were slightly decreased in livers of SHP^{Tg} mice only (Figure 5A). Protein levels of total and phosphorylated STAT1, total JAK1 (receptor to activate STAT1), total and phosphorylated mTOR and its pathway components (Rictor, Raptor, and GβL), and nuclear and cytoplasm nuclear factor-Kappa B (NF-κB), were not changed in these mice except for reduced phosphorylated JAK1 in FXR deficient mice (Figure 5B, 5C, 5D).

It is clear that STAT3 is activated by FXR deficiency. Therefore, we determined the mRNA levels of several STAT3 target genes, *c-Myc*, *p21*, *Survivin and Socs3* (Yu et al., 2009), in livers of all genotypes at 3, 6, 12 and 18 months. As anticipated, the mRNA levels of *c-Myc*, *p21* and *Survivin*, but not *Socs3*, were induced in $FXR^{-/-}$ and $FXR^{-/-}/SHP^{Tg}$ mice (Figure 6A). *Socs3*, a feedback inhibitor of the JAK2/STAT3 pathway, were slightly decreased in livers of $FXR^{-/-}$ and $FXR^{-/-}/SHP^{Tg}$ mice. STAT3 is known to be activated by IL-6, and the increased bile acids following FXR deficiency is known to induce inflammation. Thereby, we have measured the IL-6 protein levels in serum in 3-, 6-, 12- and 18-month old WT, SHP^{Tg} and $FXR^{-/-}$ mice and the results showed that at all ages, the FXR deficiency increased IL-6 levels in the serum (Figure 6B), and at 3-month old, deficiency of FXR also tended to increase IL-6 levels in the liver without statistical significance (Figure 6B). We then measured the mRNA levels of IL-1β and IL-6, as well as IL-1α. There was no change in the mRNA levels of IL-1α (data not shown), but increased levels of IL-1β and IL-6 were associated with FXR deficiency (Figure 6C).

Discussion

In the present study, we have tested the hypothesis that deficiency of SHP contributes to the HCC development in $FXR^{-/-}$ mice and increase in SHP expression in $FXR^{-/-}$ mouse livers reduces liver tumorigenesis. The results showed that overexpression of SHP did not reduce tumor incidence or tumor size, but reduced tumor malignancy, likely through enhanced apoptosis. FXR deficiency increased bile acid and IL-6 levels, as well as JAK2/STAT3 activation, which is likely a mechanism contributing to HCC development following FXR deficiency. Together, these findings reveal that molecular mechanisms of spontaneous carcinogenesis in livers of $FXR^{-/-}$ mice are not only due to decreased SHP expression, but

also due to activation of cell proliferation pathway(s) following cell injury and inflammation.

Both $FXR^{-/-}$ and $SHP^{-/-}$ mice develop spontaneous liver tumors (He et al., 2008; Kim et al., 2007; Yang et al., 2007; Zhang et al., 2008). SHP is a well-known FXR target gene (Guo et al., 2003), and over-expression of SHP inhibits HCC foci formation and arrests HCC tumor growth in xenografted nude mice models (He et al., 2008; Zhang et al., 2008). Therefore, over-expression of SHP in livers of $FXR^{-/-}$ mice was used to determine if SHP deficiency is a major mechanism leading to HCC development in $FXR^{-/-}$ mice. In this study, although the $FXR^{-/-}/SHP^{Tg}$ mice had similar tumor incidence and tumor size compared to $FXR^{-/-}$ mice, pathology analysis revealed that $FXR^{-/-}/SHP^{Tg}$ mice had fewer dysplasia/HCC cells, less bile ductular proliferation and less portal/parenchymal inflammatory cell infiltration in the liver than $FXR^{-/-}$ mice had. Arginase-1 immunostaining was stronger in $FXR^{-/-}$ mouse livers than in $FXR^{-/-}/SHP^{Tg}$ mouse livers at 18-month old. Arginase-1 has proven to be a new immunohistochemical marker in HCC and is highly expressed in HCC progression (Timek et al., 2012; Yan et al., 2010). These results indicate that SHP may partially protect $FXR^{-/-}$ mice from the HCC formation by reducing tumor malignancy. Thus, our current results indicate that overexpression of SHP does not prevent tumor initiation and promotion but likely reduces tumor progression.

The current study showed that CyclinD1 expression was induced only in livers of old $FXR^{-/-}$ mice. Despite that SHP inhibits CyclinD1 expression *in vitro* (Zhang et al., 2008), our study showed that overexpression of SHP *in vivo* did not affect CyclinD1 levels. Instead, a previous study reported that Wnt-β-catenin activated CyclinD1 in $FXR^{-/-}$ mice (Wolfe et al., 2011). Therefore, the lack of Cyclin D1 induction may be a reflection of multifaceted regulation of Cyclin D1 following FXR deletion. Consistent with previous observations (Kim et al., 2007; Zhang et al., 2008), increased apoptosis were detected in livers of $FXR^{-/-}$ and SHP^{Tg} mice. In addition, despite a similar trend of reduction of apoptosis with aging in livers of $FXR^{-/-}$ and $FXR^{-/-}/SHP^{Tg}$ mice, more apoptotic cells were found in aged $FXR^{-/-}/SHP^{Tg}$ than in $FXR^{-/-}$ mice. This relatively higher degree of apoptosis likely is a main mechanism contributing to the reduced malignancy of HCC in $FXR^{-/-}/SHP^{Tg}$ mice.

However, both $FXR^{-/-}$ and $FXR^{-/-}/SHP^{Tg}$ mice showed similarly high tumor incidence (100% at 18 months of age), similar tumor size, marked increase in liver/body weight ratio, and serum ALT activity and bile acid levels. The hepatocyte proliferation index was also similar between $FXR^{-/-}$ and $FXR^{-/-}/SHP^{Tg}$ mice. Furthermore, JAK2/STAT3 was specifically activated in livers of $FXR^{-/-}$ and $FXR^{-/-}/SHP^{Tg}$ mice as early as 3 months of age, without showing signs of JAK1/STAT1, mTOR, or NF-κB activation. While we were preparing this manuscript, a recent publication showed inhibition of STAT3 activaty following FXR activation *in vitro*, which confirmed our results (Xu et al., 2012). We further showed that STAT3 target genes, including *c-Myc*, *p21* and *Survivin*, were induced in livers of $FXR^{-/-}$ mice. These results showed that the JAK2/STAT3 pathway is activated by FXR deficiency, which is not prevented by SHP overexpression. Consistent activation of JAK2/STAT3 signaling pathway may serve as a mechanism of liver carcinogenesis in $FXR^{-/-}$ mice.

Increased inflammatory cytokines, especially IL-6, have been shown to activate STAT3. FXR deficiency is known to increase levels of bile acids, which may lead to cell injury and inflammation. Indeed, mRNA levels of the inflammatory genes, *IL-1β* and *IL-6*, were induced in livers of $FXR^{-/-}$ and $FXR^{-/-}/SHP^{Tg}$ mice with aging. It is likely that elevated bile acids induce IL-6, which in turn activates STAT3. IL-6 is a potent inflammatory cytokine playing a critical role in carcinogenesis (Naugler and Karin, 2008), and its levels were dramatically increased in HCC patients with higher IL-6 levels associated with primary liver cancer progression (Porta et al., 2008). Our results showed no activation of JAK1/STAT1, but the JAK2/STAT3 signaling pathway was consistently activated in livers of $FXR^{-/-}$ mice. STAT3, which is most commonly activated by IL-6, serves as a crucial regulator of inflammation and carcinogenesis (Wang et al., 2011). Moreover, STAT3 works as a point of convergence of numerous oncogenic signaling pathways during HCC development (Wang et al., 2011; Yu et al., 2009). Upon activation, STAT3 induces the transcription of target genes crucial for cell proliferation. We showed that *c-Myc*, *P21* and *survivin*, target genes of STAT3, were highly induced, especially in livers of aging $FXR^{-/-}$ mice. These results demonstrate that increased bile acids and IL-6 may contribute to activating the JAK2/STAT3 pathway in $FXR^{-/-}$ mice. Survivin belongs to the inhibitor of apoptosis protein (IAP) family, which inhibits caspases and blocks cell death. Studies have found that survivin is highly expressed in cancer and is associated with a poorer clinical outcome. In $FXR^{-/-}$ mice, survivin expression has been increased with aging, and overexpression of SHP could reduce the expression levels of survivin. These results indicate that SHP may induce apoptosis through inhibition the activation of survivin.

Collectively, our results demonstrate that SHP does not prevent FXR deficiency-induced HCC incidence and size, but significantly reduces tumor malignancy, indicating that overexpression of SHP may reduce tumor progression. Furthermore, the mechanism by which SHP protects from liver tumor progression may likely due to enhanced apoptosis. FXR deficiency increases bile acid levels, which may be a fundamental factor to induce inflammation, cell proliferation, and liver tumorigenesis.

Supplementary Material

Refer to Web version on PubMed Central for supplementary material.

Acknowledgments

This study was supported by the NIH fund [DK081343 & DK090036 (GLG)].

List of Abbreviations

ALT	alanine aminotransferase
GP130	glycoprotein 130
JAK	Janus kinases
FXR	farnesoid X receptor

FXR$^{-/-}$	FXR knockout
HCC	hepatocellular carcinoma
IL-1α	interleukin-1α
IL-1β	interleukin-1β
IL-6	interleukin-6
Q-PCR	quantitative real-time PCR
SOCS3	suppressor of cytokine signaling 3
SHP	small heterodimer partner
SHP$^{-/-}$	SHP knockout
SHP^{Tg}	SHP transgenic
WT	wild type

References

Cameron R, Imaida K, Ito N. Promotive effects of deoxycholic acid on hepatocarcinogenesis initiated by diethylnitrosamine in male rats. Gann. 1981; 72:635–636. [PubMed: 6118313]

Chen T, Xie G, Wang X, Fan J, Qiu Y, Zheng X, Qi X, Cao Y, Su M, Wang X, Xu LX, Yen Y, Liu P, Jia W. Serum and Urine Metabolite Profiling Reveals Potential Biomarkers of Human Hepatocellular Carcinoma. Molecular & Cellular Proteomics. 2011:10.

El-Serag HB. Hepatocellular carcinoma. N Engl J Med. 2011; 365:1118–1127. [PubMed: 21992124]

Guo GL, Lambert G, Negishi M, Ward JM, Brewer HB Jr, Kliewer SA, Gonzalez FJ, Sinal CJ. Complementary roles of farnesoid X receptor, pregnane X receptor, and constitutive androstane receptor in protection against bile acid toxicity. J Biol Chem. 2003; 278:45062–45071. [PubMed: 12923173]

He N, Park K, Zhang Y, Huang J, Lu S, Wang L. Epigenetic inhibition of nuclear receptor small heterodimer partner is associated with and regulates hepatocellular carcinoma growth. Gastroenterology. 2008; 134:793–802. [PubMed: 18325392]

Kim I, Morimura K, Shah Y, Yang Q, Ward JM, Gonzalez FJ. Spontaneous hepatocarcinogenesis in farnesoid X receptor-null mice. Carcinogenesis. 2007; 28:940–946. [PubMed: 17183066]

Li G, Guo GL. Role of Class II nuclear receptors in liver carcinogenesis. Anti-cancer agents in medicinal chemistry. 2011; 11:529–542. [PubMed: 21554208]

Li G, Thomas AM, Hart SN, Zhong X, Wu D, Guo GL. Farnesoid X receptor activation mediates head-to-tail chromatin looping in the Nr0b2 gene encoding small heterodimer partner. Mol Endocrinol. 2010; 24:1404–1412. [PubMed: 20444884]

Makishima M, Okamoto AY, Repa JJ, Tu H, Learned RM, Luk A, Hull MV, Lustig KD, Mangelsdorf DJ, Shan B. Identification of a nuclear receptor for bile acids. Science. 1999; 284:1362–1365. [PubMed: 10334992]

Maran RRM, Thomas A, Roth M, Sheng Z, Esterly N, Pinson D, Gao X, Zhang Y, Ganapathy V, Gonzalez FJ, Guo GL. Farnesoid X receptor deficiency in mice leads to increased intestinal epithelial cell proliferation and tumor development. J Pharmacol Exp Ther. 2009; 328:469–477. [PubMed: 18981289]

Meng Z, Wang X, Gan Y, Zhang Y, Zhou H, Ness CV, Wu J, Lou G, Yu H, He C, Xu R, Huang W. Deletion of IFNgamma enhances hepatocarcinogenesis in FXR knockout mice. J Hepatol. 2012; 57:1004–1012. [PubMed: 22728874]

Naugler WE, Karin M. The wolf in sheep's clothing: the role of interleukin-6 in immunity, inflammation and cancer. Trends Mol Med. 2008; 14:109–119. [PubMed: 18261959]

Parks DJ, Blanchard SG, Bledsoe RK, Chandra G, Consler TG, Kliewer SA, Stimmel JB, Willson TM, Zavacki AM, Moore DD, Lehmann JM. Bile acids: natural ligands for an orphan nuclear receptor. Science. 1999; 284:1365–1368. [PubMed: 10334993]

Porta C, De Amici M, Quaglini S, Paglino C, Tagliani F, Boncimino A, Moratti R, Corazza GR. Circulating interleukin-6 as a tumor marker for hepatocellular carcinoma. Ann Oncol. 2008; 19:353–358. [PubMed: 17962206]

Sinal CJ, Tohkin M, Miyata M, Ward JM, Lambert G, Gonzalez FJ. Targeted disruption of the nuclear receptor FXR/BAR impairs bile acid and lipid homeostasis. Cell. 2000; 102:731–744. [PubMed: 11030617]

Timek DT, Shi J, Liu H, Lin F. Arginase-1, HepPar-1, and Glypican-3 are the most effective panel of markers in distinguishing hepatocellular carcinoma from metastatic tumor on fine-needle aspiration specimens. American journal of clinical pathology. 2012; 138:203–210. [PubMed: 22904131]

Wang H, Chen J, Hollister K, Sowers LC, Forman BM. Endogenous bile acids are ligands for the nuclear receptor FXR/BAR. Mol Cell. 1999; 3:543–553. [PubMed: 10360171]

Wang H, Lafdil F, Kong X, Gao B. Signal transducer and activator of transcription 3 in liver diseases: a novel therapeutic target. International journal of biological sciences. 2011; 7:536–550. [PubMed: 21552420]

Wolfe A, Thomas A, Edwards G, Jaseja R, Guo GL, Apte U. Increased activation of the Wnt/beta-catenin pathway in spontaneous hepatocellular carcinoma observed in farnesoid X receptor knockout mice. J Pharmacol Exp Ther. 2011; 338:12–21. [PubMed: 21430080]

Xu Z, Huang G, Gong W, Zhou P, Zhao Y, Zhang Y, Zeng Y, Gao M, Pan Z, He F. FXR ligands protect against hepatocellular inflammation via SOCS3 induction. Cellular Signalling. 2012; 24:1658–1664. [PubMed: 22560881]

Yan BC, Gong C, Song J, Krausz T, Tretiakova M, Hyjek E, Al-Ahmadie H, Alves V, Xiao SY, Anders RA, Hart JA. Arginase-1: a new immunohistochemical marker of hepatocytes and hepatocellular neoplasms. Am J Surg Pathol. 2010; 34:1147–1154. [PubMed: 20661013]

Yang F, Huang X, Yi T, Yen Y, Moore DD, Huang W. Spontaneous development of liver tumors in the absence of the bile acid receptor farnesoid X receptor. Cancer Res. 2007; 67:863–867. [PubMed: 17283114]

Yu H, Pardoll D, Jove R. STATs in cancer inflammation and immunity: a leading role for STAT3. Nat Rev Cancer. 2009; 9:798–809. [PubMed: 19851315]

Zhang Y, Hagedorn CH, Wang L. Role of nuclear receptor SHP in metabolism and cancer. Biochimica et Biophysica Acta (BBA) - Molecular Basis of Disease. 2011; 1812:893–908.

Zhang Y, Soto J, Park K, Viswanath G, Kuwada S, Abel ED, Wang L. Nuclear receptor SHP, a death receptor that targets mitochondria, induces apoptosis and inhibits tumor growth. Mol Cell Biol. 2010; 30:1341–1356. [PubMed: 20065042]

Zhang Y, Xu P, Park K, Choi Y, Moore DD, Wang L. Orphan receptor small heterodimer partner suppresses tumorigenesis by modulating cyclin D1 expression and cellular proliferation. Hepatology. 2008; 48:289–298. [PubMed: 18537191]

Zhu Y, Li F, Guo GL. Tissue-specific function of farnesoid X receptor in liver and intestine. Pharmacological Research. 2011; 63:259–265. [PubMed: 21211565]

Highlight

- Overexpression of SHP does not prevent HCC incidence and size in FXR KO mice but reduces malignancy
- Increased SHP promotes apoptosis
- Increased bile acid and inflammation maybe fundamental factors leading to HCC formation with FXR deficiency

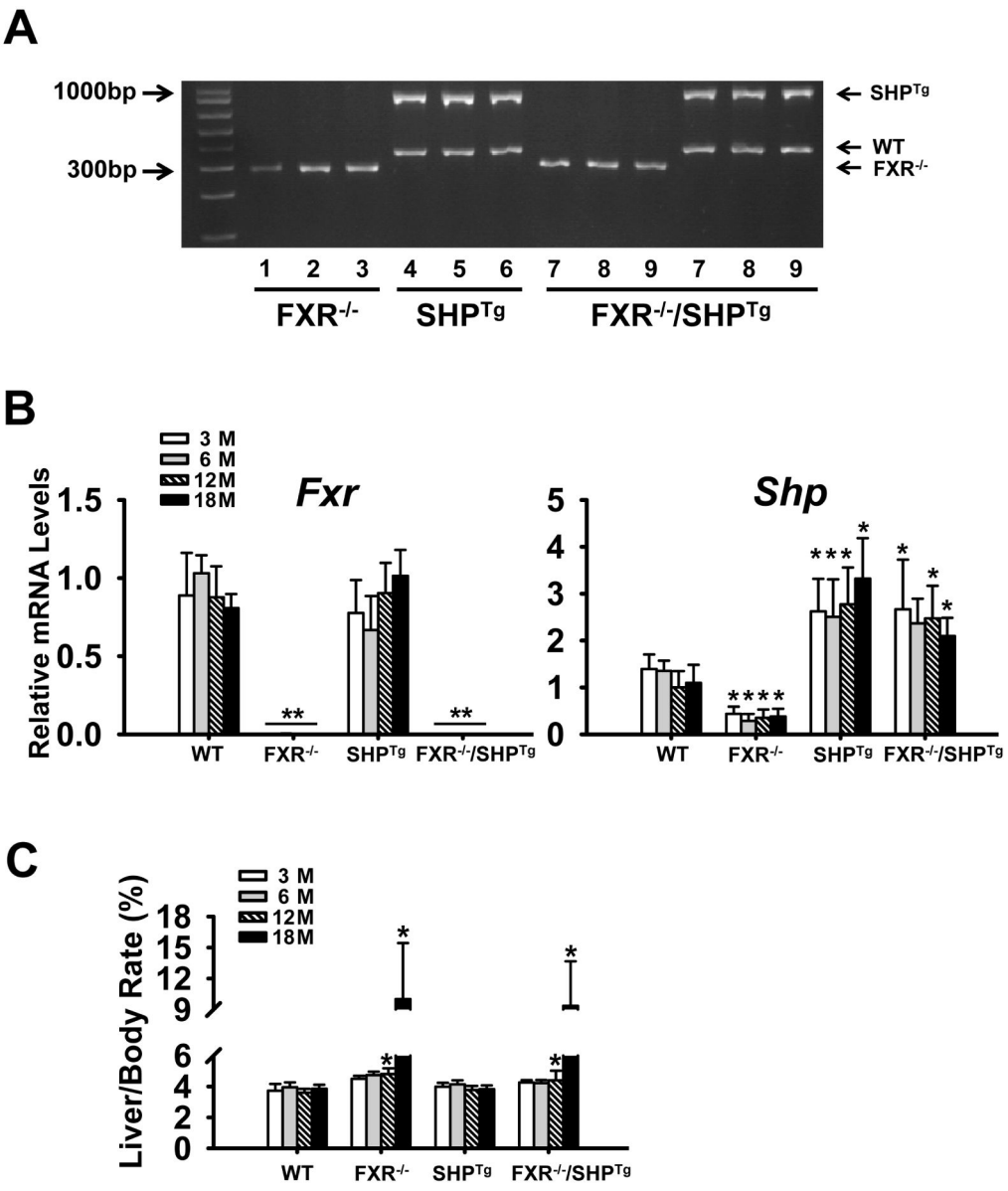

Figure 1. Generation of the FXR$^{-/-}$/SHP^{Tg} mice

FXR$^{-/-}$/SHP^{Tg} mice were generated by cross-breeding FXR$^{-/-}$ and SHP^{Tg} mice. **(A)** The correct genotypes of the mice were confirmed by PCR-based genotyping method. **(B)** The mRNA expression levels of *Fxr* and *Shp* in the livers of these mice. **(C)** The liver/body weight rate of these mice. An asterisk means $P < 0.05$, and a double asterisk means $P < 0.01$.

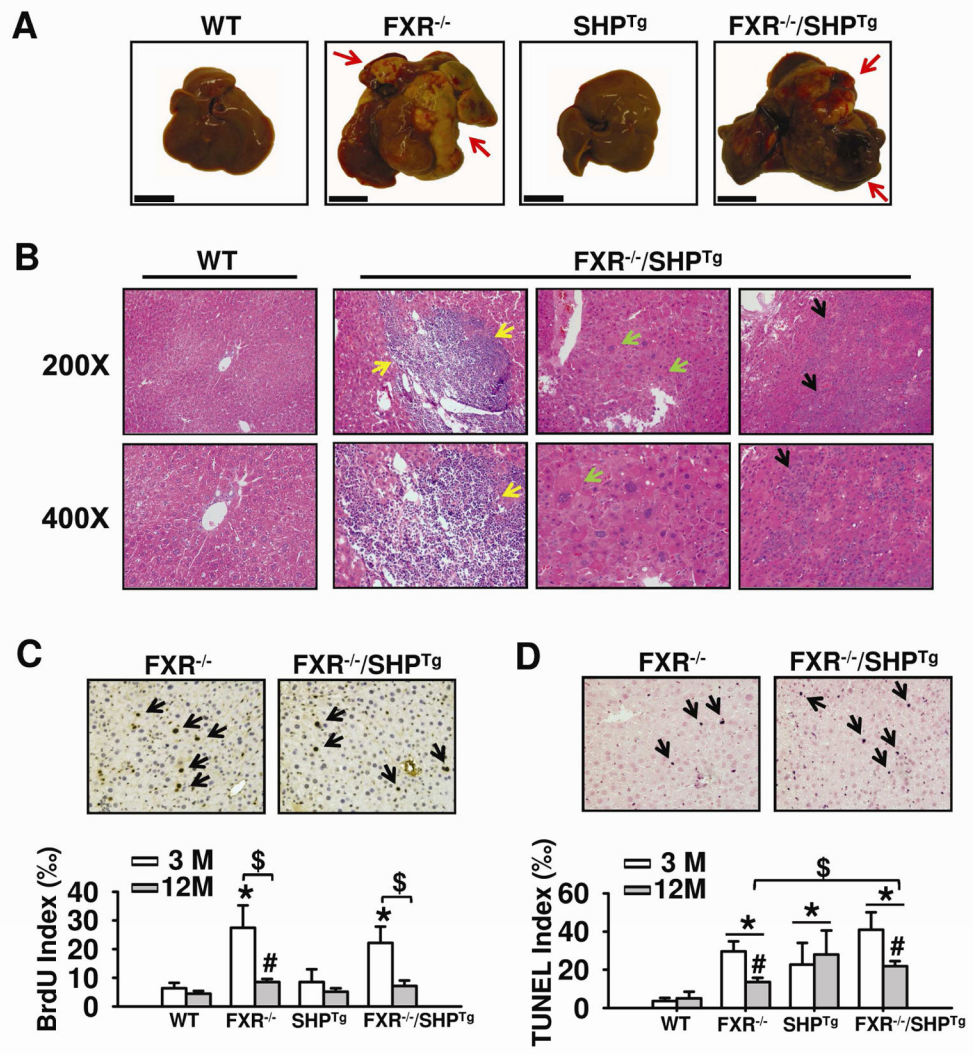

Figure 2. Liver tumor development in WT, FXR$^{-/-}$, SHP^{Tg} and FXR$^{-/-}$/SHP^{Tg} mice

(A) Representative liver morphology of WT, FXR$^{-/-}$, SHP^{Tg} and FXR$^{-/-}$/SHP^{Tg} mice at 18-month-old shows grossly identified liver tumor nodules (arrows). The scale bar indicates 1cm. **(B)** Liver H&E staining indicates portal inflammation (yellow arrows), hepatocyte dysplasia (green arrows), and HCC (black arrows). The representative pictures were from FXR$^{-/-}$/SHP^{Tg} mice at 18-month old. Magnification, 200X and 400X. **(C)** Quantification of the hepatocyte BrdU incorporation index from livers of 3- and 12-month-old mice of each genotype. The representative pictures are from livers of 3-month-old FXR$^{-/-}$ and FXR$^{-/-}$/SHP^{Tg} mice. An asterisk or pound indicates $P < 0.05$ between WT and FXR$^{-/-}$ or FXR$^{-/-}$/SHP^{Tg} groups at the same age. A dollar sign means $P < 0.05$ between 3- and 12-month-old mice of the same genotype. **(D)** Quantification of TUNEL assay results from livers of 3- and 12-month-old mice from each genotype. The representative pictures are for livers of 3-month-old FXR$^{-/-}$ and FXR$^{-/-}$/SHP^{Tg} mice. An asterisk indicates $P < 0.05$ between WT and other groups of the same age. A pound sign indicates $P < 0.05$ between 3-month and 12-month-old mice of the same genotype. A dollar sign indicates $P < 0.05$ between FXR$^{-/-}$ and FXR$^{-/-}$/SHP^{Tg} mice of the same age.

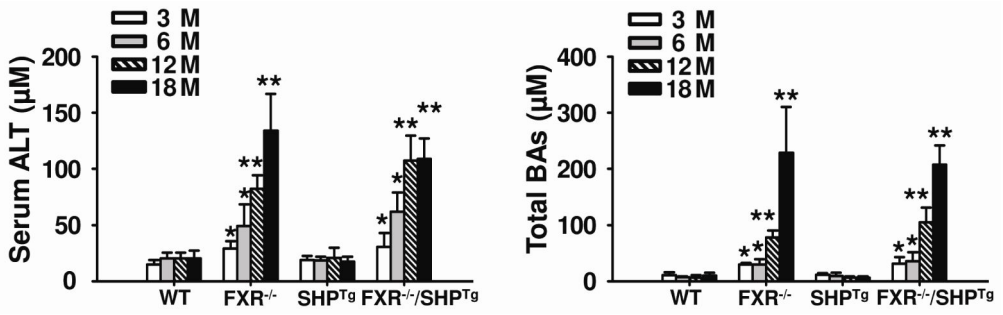

Figure 3. Serum ALT activity and serum bile acid (BA) levels

ALT activity (A) and BA levels (B) were determined by commercially available kits in WT, $FXR^{-/-}$, SHP^{Tg} and $FXR^{-/-}/SHP^{Tg}$ mice at 3-, 6-, 12- and 18-month old. An asterisk indicates $P < 0.05$ and double asterisks indicate $P < 0.01$ between WT and $FXR^{-/-}$ or $FXR^{-/-}/SHP^{Tg}$ mice.

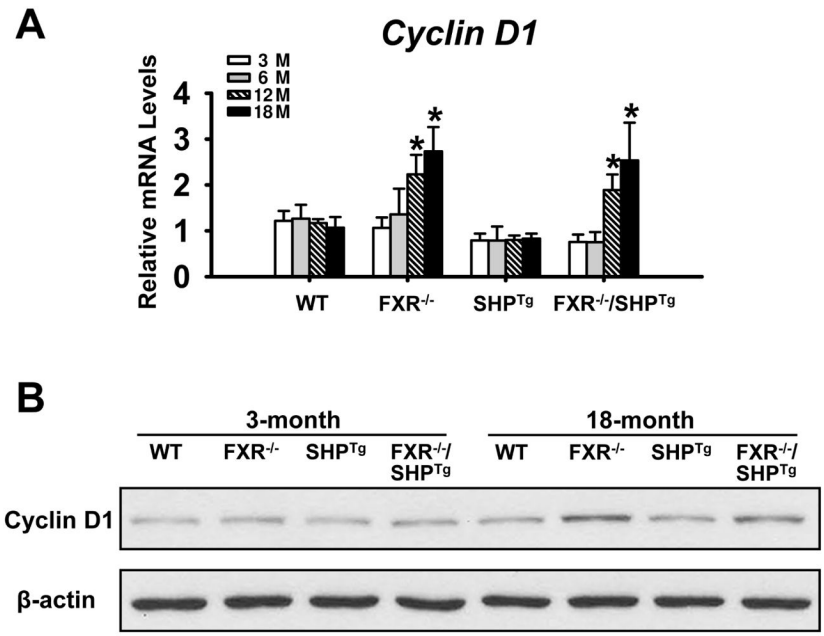

Figure 4. The mRNA and protein expressions of Cyclin D1

(A) The Cyclin D1 mRNA levels were determined by the Q-PCR method in WT, $FXR^{-/-}$, SHP^{Tg} and $FXR^{-/-}/SHP^{Tg}$ mice at 3-, 6-, 12- and 18-month old. **(B)** The protein levels of Cyclin D1 were determined in WT, $FXR^{-/-}$, SHP^{Tg} and $FXR^{-/-}/SHP^{Tg}$ mice at 3- and 18-month old. An asterisk indicates $P < 0.05$.

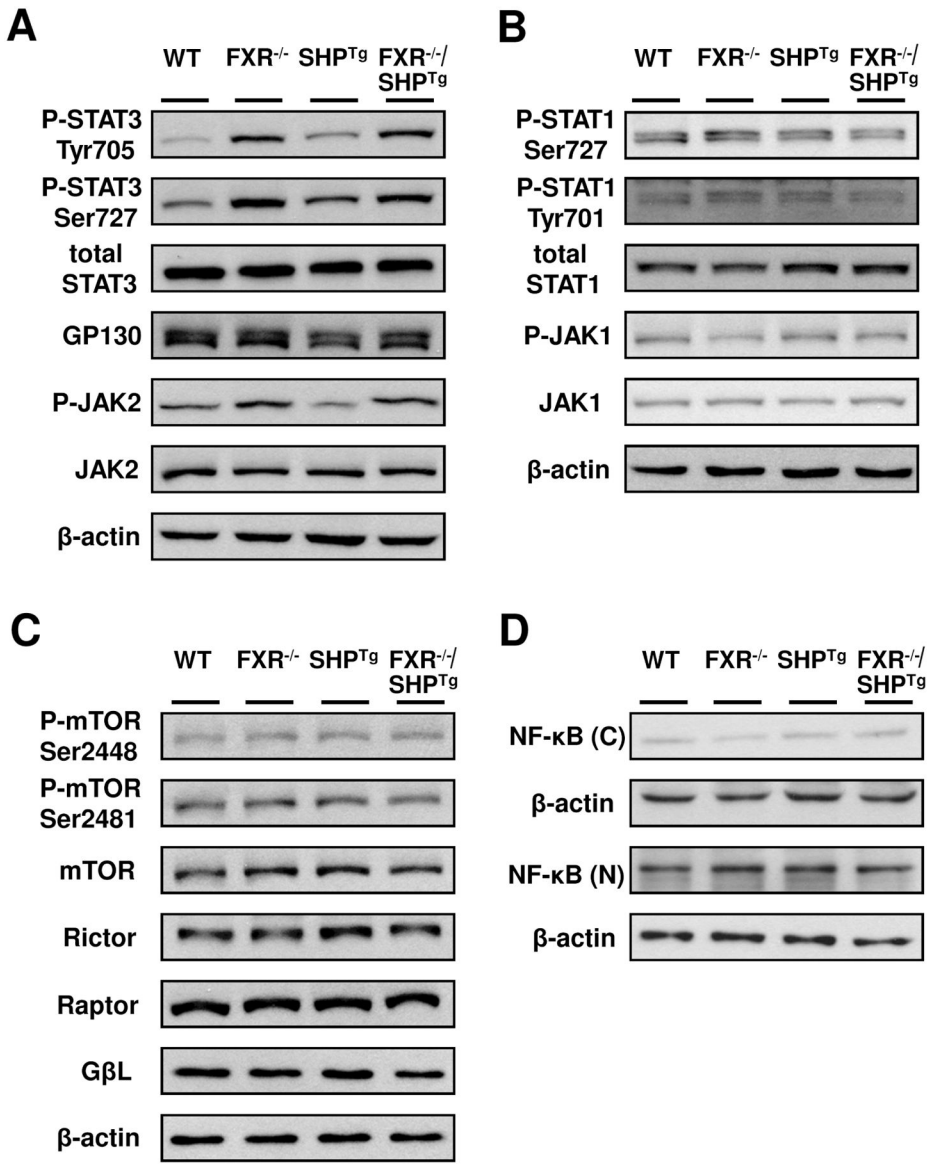

Figure 5. STAT3, but not STAT1, mTOR or NF-κB was activated in livers of FXR$^{-/-}$ and FXR$^{-/-}$/SHP^{Tg} mice

Western Blot analysis of total hepatic protein levels from 3-month-old WT, FXR$^{-/-}$, SHP^{Tg} and FXR$^{-/-}$/SHP^{Tg} mice. **(A)** Representative results of phosphorylated STAT3, total STAT3, GP130, phosphorylated JAK2, and total JAK2. **(B)** Phosphorylated STAT1, total STAT1, phosphorylated JAK1, and total JAK1. **(C)** Phosphorylated mTORs, total mTOR, Rictor, Raptor, and GβL. **(D)** Hepatic cytoplasmic and nuclear protein levels of NF-κB in 3-month-old WT, FXR$^{-/-}$, SHP^{Tg} and FXR$^{-/-}$/SHP^{Tg} mice. Each band represents a pooled sample from 3 individual mice with the same genotype, and β-actin levels were used as internal loading control.

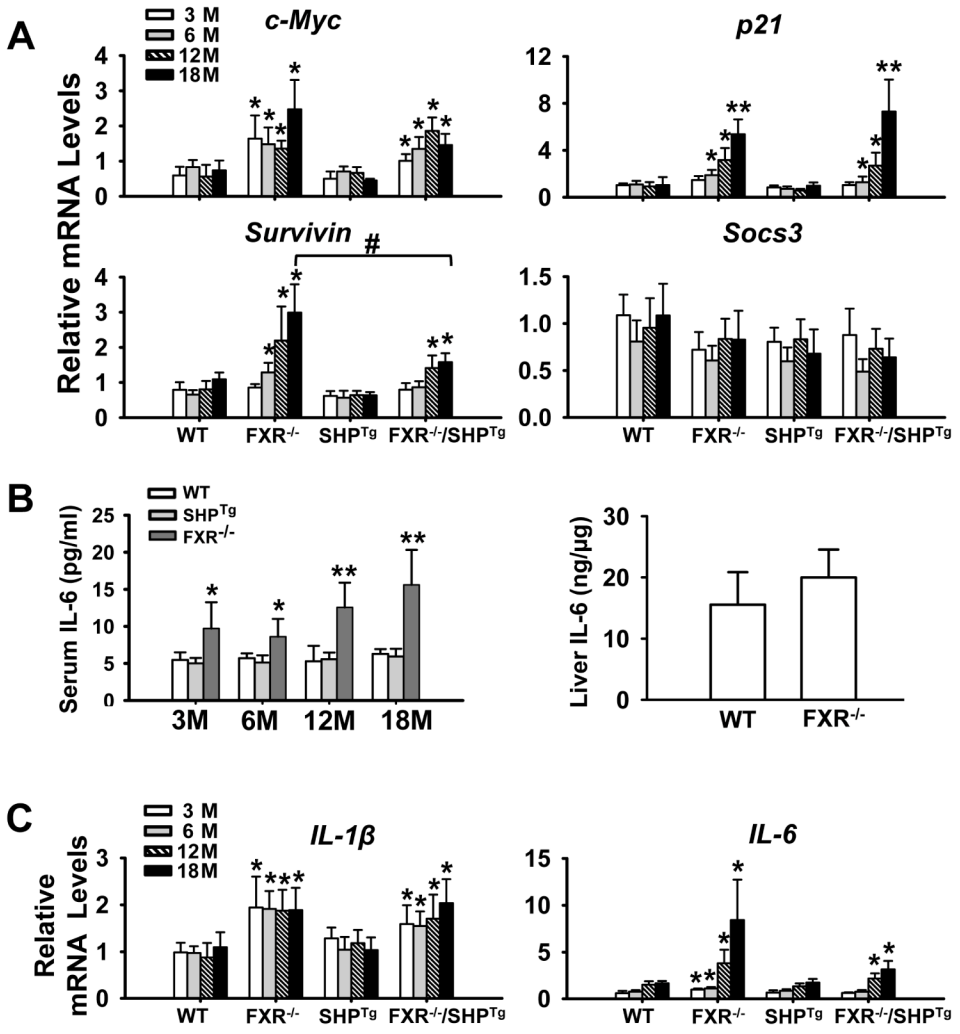

Figure 6. Activation of JAK2/STAT3 signaling pathway in livers of WT, $FXR^{-/-}$, SHP^{Tg}, and $FXR^{-/-}/SHP^{Tg}$ mice at 3-, 6-, 12-, and 18-month old

(A) Q-PCR analysis of mRNA expression levels of STAT3 downstream target genes, *c-Myc*, *p21*, *Survivin*, and *Socs3*. **(B)** Serum IL-6 levels in WT, SHP^{Tg} and $FXR^{-/-}$ mice at 3-, 6-, 12- and 18-month old; liver IL-6 protein levels in WT and $FXR^{-/-}$ mice at 3-month old. **(C)** Q-PCR analysis of mRNA expression levels of IL-1β and IL-6 in livers of each genotype at 3-, 6-, 12- and 18-month old. An asterisk indicates $P < 0.05$ and double asterisks mean $P < 0.01$ between WT and $FXR^{-/-}$ or $FXR^{-/-}/SHP^{Tg}$ mice.

Table 1

Tumor incidence in 12- and 18-month old mice

	12-month old		18-month old	
Group	**Mouse number**	**Tumor incidence (%)**	**Mouse number**	**Tumor incidence (%)**
WT	16	0	18	0
$FXR^{-/-}$	16	56.3	20	100
SHP^{Tg}	16	0	18	0
$FXR^{-/-}SHP^{Tg}$	14	64.3	18	100

Note: Mice in each group were sacrificed at 12 and 18 months of age with n=14–20 per group.

Table 2

Summarized results of pathology for 18-month old male mice

Groups	Rate of HCC or dysplasia (tumor early stage)	Rate of inflammation (portal)	Rate of inflammation (parenchymal)	Rate of bile ductular proliferation	Rate of necrosis
Wild Type (n=6)	N/A	N/A	N/A	N/A	N/A
FXR Knockout (n=10)	HCC (5/10), high grade dysplasia (5/10)	portal inflammation (6/10): mild (2/10), moderate (1/10), or marked (3/10)	parenchymal inflammaiton (3/10): mild (1/10) or marked (2/10)	2/10	3/10
SHP Transgenic (n=8)	N/A	N/A	N/A	N/A	N/A
FXR Knockout/SHP Transgenic (n=9)	HCC (5/9), high grade dysplasia (1/9), low grade dysplasia (3/9)	portal inflammation (4/9): mild (2/9), moderate (1/9), or marked (1/9)	N/A	1/9	1/9